

Structural and electronic properties of PbSe nanocrystals from first principles

A. Franceschetti

National Renewable Energy Laboratory, Golden, Colorado 80401, USA

(Received 25 March 2008; revised manuscript received 3 June 2008; published 14 August 2008)

This work reports density-functional calculations of the structural and electronic properties of PbSe nanocrystals ranging in radius from 8.4 to 14.8 Å. We considered nearly spherical, rocksalt-structure nanocrystals with 1:1 Pb:Se stoichiometry and no molecular species adsorbed at the surface. We found that: (i) The Pb-Se bond lengths and bond angles are significantly distorted compared to those in bulk PbSe, in an ~ 8 -Å-thick shell near the surface of the nanocrystal. (ii) Even in the absence of surface passivants, there are no surface states in the band gap of the nanocrystals. (iii) The nanocrystal band gap undergoes a significant redshift (Franck-Condon shift) when an electron is promoted from the valence band to the conduction band. For nanocrystals of radius $R=8.4$ Å, the calculated Franck-Condon shift is ~ 0.18 eV. (iv) The calculated electronic density of states shows a significant asymmetry between valence and conduction states, suggesting that the postulated “mirror symmetry” between valence band and conduction band does not exist.

DOI: [10.1103/PhysRevB.78.075418](https://doi.org/10.1103/PhysRevB.78.075418)

PACS number(s): 73.22.Dj, 61.46.Hk

I. INTRODUCTION

The potential application of semiconductor quantum dots as light absorbers in third-generation solar-cell devices has attracted considerable interest in recent years, particularly after the discovery^{1,2} of efficient multiple-exciton generation in PbSe and PbS nanocrystals (NCs). This phenomenon, which was later reported also in CdSe,³ PbTe,⁴ InAs,^{5,6} and Si (Ref. 7) NCs, opens up the possibility of generating multiple electron-hole pairs from a single, high-energy photon, thereby potentially increasing solar-cell efficiency. The use of semiconductor NCs for solar-energy conversion requires a good match between the NC absorption spectrum and the solar spectrum. Taking into account that quantum-confinement effects tend to open up the band gap, NCs made of narrow-gap semiconductors—such as lead chalcogenides, group-III antimonides, Ge, and InAs—are potentially more suitable for solar-cell applications. Among those, PbSe NCs have received perhaps the most attention, both experimentally^{8–23} and theoretically.^{24–38}

Bulk PbSe has unique structural and electronic properties, which in turn are expected to lead to unusual properties in PbSe NCs:

(i) PbSe has a strong ionic character and crystallizes in the rocksalt lattice structure. This is expected to lead to different surface properties and different equilibrium shapes of PbSe NCs compared to those of other semiconductor NCs.

(ii) Both the valence-band and conduction-band edges of bulk PbSe are located at the L point of the fcc Brillouin zone and are therefore fourfold degenerate (eightfold degenerate including spin). In PbSe NCs, such degeneracy is lifted by intervalley and intraband couplings, induced by the lack of translational symmetry. However, the resulting energy splittings are expected to be small compared to the energy-level spacings. Thus, the band edges are expected to retain their high degeneracy.

(iii) The electron and hole effective masses of bulk PbSe are rather small: $m_h^\perp=0.034m_0$, $m_h^\parallel=0.068m_0$, $m_e^\perp=0.040m_0$, and $m_e^\parallel=0.070m_0$.³⁹ Upon quantum confinement, light effective masses are expected to lead to widely spaced energy

levels, both in the conduction band and in the valence band.

(iv) The electron and hole effective masses of bulk PbSe are similar. In PbSe NCs, this is expected to lead to a “mirrorlike symmetry” between conduction-band and valence-band density of states, whereby the manifold of valence-band energy levels is a mirror image of the conduction-band energy levels.

(v) Bulk PbSe has a large dielectric constant ($\epsilon_\infty=23$). Thus, carrier-carrier interactions are expected to be strongly screened.

These expectations have come to constitute the “standard model” of the structural and electronic properties of PbSe NCs, which has often been used to interpret and analyze experimental data.^{1,2,10,15} Some recent experimental results, however, have proved difficult to reconcile with this model. For example, the intraband electron relaxation rate is expected to be small in PbSe NCs because of the large electron level spacing [point (iii) above], which prevents efficient phonon-assisted relaxation, and the equally large hole level spacing [point (iv) above], which makes electron-hole Auger scattering⁴⁰ inconsequential for electron relaxation. Nevertheless, relatively short (~ 1 – 5 ps) electron relaxation times have been reported in PbSe NCs,^{10,15,17} raising the question of the validity of the standard model of the electronic structure of PbSe NCs.³⁸ Indeed, atomistic pseudopotential calculations³⁰ have recently shown that some of the predictions of the envelope-function approximation²⁴ result from an oversimplification of the energy-level structure. In particular, the commonly accepted predictions of mirror symmetry between valence and conduction states [point (iv)] and of large hole spacing [point (iii)] are based on the assumption of a single valence-band maximum and a single conduction-band minimum. This assumption does not take into account the fact that several valence-band maxima exist in an energy window of ~ 1 eV near the top of the valence band of PbSe,^{30,41} thereby increasing the valence-band density of states. First-principles calculations, which do not require adjustable parameters fitted to experimental results, would be particularly valuable to clarify these open issues.

Recently, time-dependent density-functional calculations of carrier relaxation rates in small PbSe clusters (up to 136

atoms) have been reported in the literature.^{35,36} Kamisaka *et al.*³⁵ calculated the vibrationally induced dephasing rates of single excitons and biexcitons in $\text{Pb}_{16}\text{Se}_{16}$ and $\text{Pb}_{68}\text{Se}_{68}$ clusters. They found that the dephasing times depends weakly on the excitation energy and are faster for multiexcitons than for single excitons. Kilina *et al.*³⁶ reported first-principles simulations of phonon-assisted relaxation of carriers in $\text{Pb}_{16}\text{Se}_{16}$ clusters with the zinc-blende lattice structure. The authors found a short, picosecond time scale for carrier relaxation, which they rationalized in terms of the relatively large electron and hole densities of states.

In this work we report density-functional calculations of the structural and electronic properties of relatively large PbSe NCs, ranging in radius from 8.4 to 14.8 Å. We consider nearly spherical, rocksalt-structure PbSe NCs with 1:1 stoichiometry and no molecular species adsorbed at the surface. We find that: (i) The Pb-Se bond lengths and bond angles are significantly distorted compared to those in bulk PbSe, in an ~ 8 -Å-thick shell near the surface of the NC. (ii) Even in the absence of surface passivants, there are no surface states in the band gap of the NCs. (iii) The band gap undergoes a significant redshift (Franck-Condon shift) when an electron is promoted from the valence band to the conduction band. For NCs of radius $R=8.4$ Å, the calculated Franck-Condon shift is ~ 0.18 eV. (iv) The calculated electronic density of states shows a significant asymmetry between valence and conduction states, suggesting that the postulated mirror symmetry between valence and conduction manifolds does not exist.

II. METHOD

The calculations were performed using density-functional theory in the generalized-gradient approximation.⁴² The Perdew-Burke-Ernzerhof (PBE) energy functional⁴³ was used to approximate the exchange-correlation energy. Electron-ion interactions were described using the projector-augmented wave method,⁴⁴ and the electron wave functions were expanded in a plane-wave basis set with an energy cutoff $E_{\text{cut}}=212$ eV. Periodic boundary conditions were enforced by considering a cubic array of PbSe NCs, separated by a sufficiently large region of vacuum to effectively decouple the NC wave functions. Spin-orbit coupling was not included in the calculations. Spin-orbit effects lead to energy-level splittings both in the valence band and in the conduction band.⁴¹ They are therefore important for the spectroscopy of NCs. However, they have only a minor effect on the structural properties of bulk PbSe,⁴⁵ and we expect the same to be true for PbSe NCs.

To determine the ground-state geometry, all atomic positions were relaxed according to the quantum-mechanical forces acting on the atoms. The excited-state geometry was calculated by promoting one electron from the highest occupied molecular orbital (HOMO) to the lowest unoccupied molecular orbital (LUMO) of the NC and keeping the electronic configuration fixed while relaxing the atomic positions.⁴⁶ This approach provides a good approximation for the excited-state geometry of the NCs.⁴⁶ Detailed first-principles calculations for *bulk* PbSe—using PBE and other

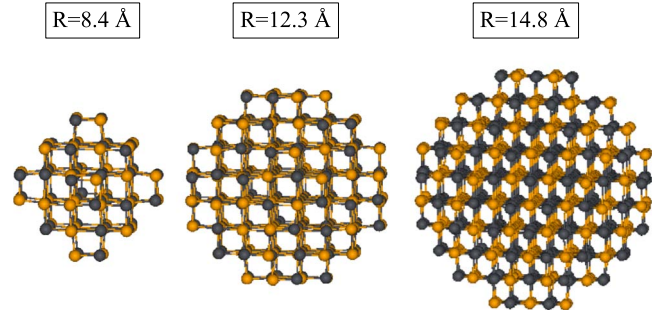


FIG. 1. (Color online) Atomistic structure of three PbSe NCs of different sizes. The dark circles denote Pb atoms and the light circles, Se atoms. The atoms have been fully relaxed to their equilibrium positions.

energy functionals—were presented in Ref. 47.

We have considered nearly spherical PbSe NCs ranging in size (radius) from 8.4 to 14.8 Å. The initial atomic configuration of the NCs was constructed by cutting a spherical segment from bulk PbSe in the rocksalt lattice structure, centered halfway between a Pb atom and one of the neighboring Se atoms. The resulting NCs are stoichiometric (equal numbers of Pb and Se atoms) by construction. The NC diameter R was derived from the number of atoms, N , as $R=(3N/32\pi)^{1/3}a_0$, where $a_0=6.21$ Å is the calculated bulk lattice constant. No passivating species were added at the surface of the NCs. Indeed, it is well known that because of the ionic character of the Pb-Se chemical bond, the PbSe [001] surface is free from gap states.⁴⁸ The surfaces of stoichiometric PbSe NCs are also expected to be free from gap states, as discussed in Refs. 28, 35, and 36. We have also considered nonstoichiometric PbSe NCs, following the results of recent mass-spectroscopy measurements by Moreels *et al.*,²¹ which showed that the surface of PbSe NCs is Pb rich. However, we found that in the absence of passivation, Pb-rich NCs have a large density of states in the band gap.

III. STRUCTURAL PROPERTIES

Figure 1 shows the calculated equilibrium geometry of three PbSe NCs: $\text{Pb}_{44}\text{Se}_{44}$ (radius $R=8.4$ Å), $\text{Pb}_{140}\text{Se}_{140}$ ($R=12.3$ Å), and $\text{Pb}_{240}\text{Se}_{240}$ ($R=14.8$ Å). Although the Pb and Se atoms in the NCs retain the cubic coordination of the rocksalt lattice structure, the Pb-Se bond lengths and bond angles are significantly distorted compared to those in bulk PbSe. This is illustrated more clearly in Fig. 2, which shows, for each of the three NCs of Fig. 1, the length of the Pb-Se bonds as a function of the distance of the bonds from the center of the NC. The Pb-Se bond lengths are close to the bulk equilibrium bond length (calculated value: $d=3.103$ Å) near the center of the NCs, whereas they deviate significantly from the bulk value as the surface is approached. Specifically, in an ~ 8 -Å-thick shell near the surface the bond lengths follow a bimodal distribution (see Fig. 2), with values ranging from ~ 2.7 Å (-12% deviation from the bulk equilibrium bond length) to ~ 3.6 Å ($+16\%$ deviation). However, in the presence of surface passivants, the deviations from the bulk equilibrium bond length are expected to

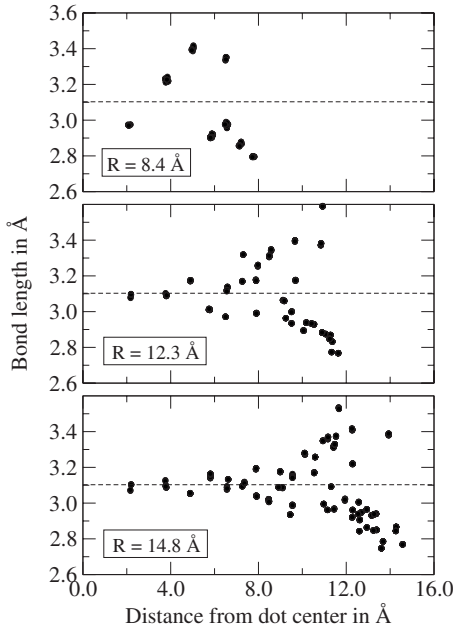


FIG. 2. Ground-state bond-length distribution of PbSe NCs. For each Pb-Se bond, the corresponding bond length is shown as a function of the distance of the bond from the geometric center of the NC. The dashed lines indicate the calculated *bulk* Pb-Se bond length ($d=3.103$ Å).

be smaller.⁴⁹ Interestingly, significant bond-length variations (on the order of $\pm 10\%$ with respect to the bulk bond length) have been experimentally observed⁵⁰ and theoretically predicted⁵¹ for the PbTe (001) surface and have been attributed to a combination of surface relaxation and surface “rumpling.” A similar effect was recently reported in the case of the (001) surface of PbSe.⁵²

The average Pb-Se bond length of the NC in the ground-state geometry (d_{av}) is slightly smaller than the bulk equilibrium bond length and decreases as the size decreases: $d_{av} = 3.030, 3.063, \text{ and } 3.078$ Å for $R=8.4, 12.3, \text{ and } 14.8$ Å, respectively. Note that a simple ionic model of the NCs, in which the surface energy is estimated using the Madelung model, would predict an *increase* in the average lattice parameter with decreasing NC size,⁵³ in contrast with the present calculations.

The formation energy of a PbSe NC is given by $\Delta E_F = E_{NC} - N\varepsilon_{bulk}$, where E_{NC} is the total energy of the NC, ε_{bulk} is the total energy per atom of *bulk* PbSe, and N is the total number of Pb and Se atoms in the NC. The formation energy can be further decomposed into a surface contribution and a relaxation contribution:

$$\Delta E_F = \Delta E_{surf} + \Delta E_{rlx}. \quad (1)$$

Here ΔE_{surf} is the formation energy of the NC calculated with the atoms fixed at their equilibrium bulk positions, so it accounts for the increase in energy due to the broken bonds at the surface of the NC. ΔE_{rlx} is the energy gain due to atomic relaxations both at the surface and in the interior of the NC. The calculated values of ΔE_{surf} , ΔE_{rlx} , and ΔE_F are shown in Table I.

TABLE I. Calculated formation energies of PbSe NC. The total formation energy ΔE_F is decomposed into a surface contribution (ΔE_{surf}) and a relaxation contribution (ΔE_{rlx}).

Radius (Å)	ΔE_{surf} (eV/atom)	ΔE_{rlx} (eV/atom)	ΔE_F (eV/atom)
8.4	0.32	-0.14	0.18
12.3	0.23	-0.11	0.12
14.8	0.21	-0.10	0.11

We see that both the surface contribution and the relaxation contribution decrease in magnitude approximately as $1/R$ as the NC size increases, as one might expect based on the ratio between the numbers of surface and interior atoms. Indeed, the Madelung model of ionic NCs predicts a $1/R$ scaling of the surface energy with the NC radius.⁵³ However, we find that the Madelung model overestimates the surface energy ΔE_{surf} . For example, in the case of a $R=12.3$ Å NC, we find that $\Delta E_{surf}^{Mad} = 1.28$ eV/atom, compared to the *ab initio* value of 0.23 eV/atom (Table I). Thus, we conclude that simple ionic models are unable to accurately describe the structural properties of PbSe NCs.

IV. ELECTRONIC STRUCTURE

The PBE approximation correctly locates the band gap of bulk PbSe at the L point of the fcc Brillouin zone⁴⁶ but significantly underestimates its magnitude, $\varepsilon_{g,bulk}^{PBE} = -0.12$ eV,⁴⁶ compared to the experimental band gap of 0.145 eV at 4 K.³⁹ When spin-orbit coupling is neglected, the calculated band gap of bulk PbSe increases to 0.30 eV,⁴⁶ thereby overcompensating for the PBE error. A similar qualitative cancellation of errors can be expected in our PBE calculations for PbSe NCs. Table II summarizes the calculated, no-spin-orbit, uncorrected HOMO-LUMO gaps (ε_g) of the PbSe NCs considered in this work. The HOMO-LUMO gaps of the unrelaxed NCs (where the atoms are kept fixed at their ideal, bulklike positions) are also shown in Table II. Note the significant increase in the HOMO-LUMO gap upon relaxation.

To investigate the spatial localization of the band-edge wave functions, we show in Fig. 3 the projection of the band-edge states on the surface atoms (defined as atoms with coordination number smaller than 6) as a function of energy. We find that in the relaxed geometry the band-edge states are localized primarily in the interior of the NCs. When the at-

TABLE II. Calculated HOMO-LUMO gap of PbSe NCs before (ε_g^{unrlx}) and after (ε_g) atomic relaxations. The calculated Franck-Condon shift ($\Delta\varepsilon_g^{FC}$) and the difference between the absorption and emission HOMO-LUMO gaps ($\Delta\varepsilon_g^{FC}$) are also shown.

Radius (Å)	ε_g^{unrlx} (eV)	ε_g (eV)	$\Delta\varepsilon_g^{FC}$ (eV)	ΔE^{FC} (eV)
8.4	0.97	1.39	0.16	0.17
12.3	0.81	1.15	0.03	0.03
14.8	0.33	0.85	0.02	0.02

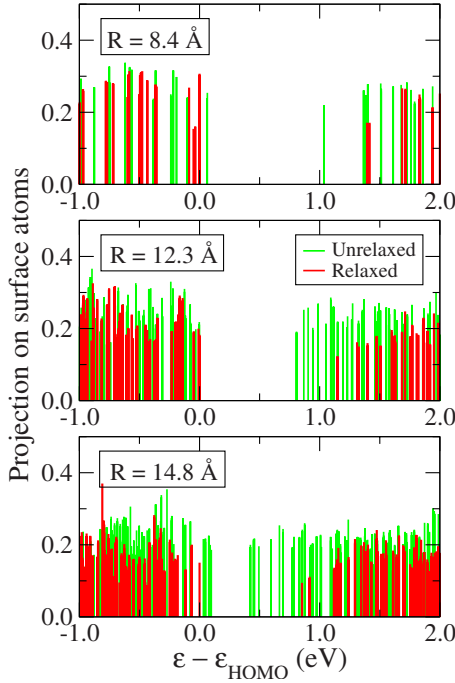


FIG. 3. (Color online) Projection of the band-edge states of PbSe NCs on the surface Pb and Se atoms. The reference energy level is the HOMO of the relaxed NCs.

oms are in their ideal, unrelaxed positions, the LUMO energy, and consequently the HOMO-LUMO gap, is significantly smaller than in the relaxed geometry (see also Table II). However, we find the LUMO—as well as the unoccupied electronic states just above the LUMO—is still mostly localized in the interior of the NC. Thus, PbSe NCs have a fundamentally different electronic structure from that of CdSe NCs, which are quasimetallic when the atoms are in their ideal, bulklike positions, and they develop a midgap state when the atoms are fully relaxed.⁵⁴

Experimental results for small PbSe NCs such as those considered here are relatively scarce. Lipovskii *et al.*⁸ measured the lowest excitonic energy of PbSe NCs embedded in a phosphate glass. They found excitonic gaps of 1.2 eV for NCs of radius $R \sim 9$ Å and 1.0 eV for $R \sim 17$ Å. Schaller *et al.*¹⁷ reported a value of 1.25 eV for the lowest-energy absorption peak of PbSe colloidal NCs of radius $R \sim 14$ Å, while Moreels *et al.*²¹ reported a band gap of 1.0 eV for quasispherical PbSe NCs of radius $R \sim 16$ Å. These results are in qualitative agreement with the present calculations (Table I), especially considering the relatively large spread of the measured gaps for NCs of similar size. Note that excitonic effects (electron-hole interactions) are relatively small in PbSe NCs because of the large dielectric screening.³⁰

The emission peak of semiconductor NCs is usually redshifted with respect to the lowest-energy absorption peak (Stokes shift). Lifshitz *et al.*¹⁶ measured the Stokes shift of PbSe NCs and PbSe/PbSe_xS_{1-x} core/shell NCs as a function of size, shell thickness, and shell composition. They reported Stokes shifts ranging from 100 meV for PbSe core NCs of diameter $D=4$ nm to -10 meV (anti-Stokes shift) for $D=6.1$ nm. Several different contributions to the Stokes shift in PbSe NCs have been discussed in the literature, including

size-distribution effects¹⁶ and electron-hole Coulomb and exchange interactions.³⁴ Here we focus on the Franck-Condon shift, which was shown to be significant in small Si NCs (Refs. 46 and 55–57) but has never been calculated for PbSe NCs. The Franck-Condon shift ΔE^{FC} was calculated from total-energy differences, as discussed in Ref. 46. Denoting by $\{\mathbf{R}_{\text{GS}}\}$ the set of equilibrium atomic positions in the electronic ground state and by $\{\mathbf{R}_{\text{XS}}\}$ the equilibrium atomic positions in the excited state, we have

$$\Delta E^{\text{FC}} = [E_{\text{XS}}(\mathbf{R}_{\text{GS}}) - E_{\text{GS}}(\mathbf{R}_{\text{GS}})] - [E_{\text{XS}}(\mathbf{R}_{\text{XS}}) - E_{\text{GS}}(\mathbf{R}_{\text{XS}})], \quad (2)$$

where E_{GS} and E_{XS} are the total energies of the NC in the ground and excited states, respectively. Alternatively, the Franck-Condon shift can be calculated as the difference between the HOMO-LUMO gap calculated at the ground-state geometry and the excited-state geometry:

$$\Delta \varepsilon_g^{\text{FC}} = \varepsilon_g(\mathbf{R}_{\text{GS}}) - \varepsilon_g(\mathbf{R}_{\text{XS}}). \quad (3)$$

The Franck-Condon shifts of PbSe NCs, calculated using both of Eqs. (2) and (3), are summarized in Table II. Note that the two approaches [Eqs. (2) and (3)] give very similar results, in contrast to the calculations of Degoli *et al.*,⁵⁶ who found significant differences between ΔE^{FC} and $\Delta \varepsilon_g^{\text{FC}}$ in the case of small Si NCs. For the $R=8.4$ Å PbSe NCs, our calculated Franck-Condon shift is 0.18 eV. For larger PbSe NCs, the calculated shift is 0.02–0.03 eV. These results suggest that the Franck-Condon effect provides a sizable contribution to the Stokes shift in small PbSe NCs. We find that the Franck-Condon shift of PbSe NCs is similar in magnitude to that of Si NCs of similar size.^{46,55}

One of the most debated aspects of the electronic structure of PbSe NCs is the existence of “mirror symmetry” between valence-band and conduction-band levels. This symmetry was initially postulated based on the similarity of the electron and hole effective masses at the L point of the bulk Brillouin zone.²⁴ Interestingly, many experimental results concerning the electronic and optical properties of PbSe NCs have been interpreted assuming the existence of such mirror symmetry. For example, Schaller *et al.*¹ explained the observed $3E_g$ photon-energy threshold for carrier multiplication by suggesting that because of the mirror symmetry of the valence and conduction states, the excess energy of the photogenerated electron-hole pair is partitioned approximately equally between the electron and the hole. Thus, only absorbed photons of energy $3E_g$ or larger can create carriers with excess energy equal to E_g , necessary to initiate carrier multiplication.¹ An *et al.*³⁰ recently disputed the assumption of mirror symmetry between valence and conduction states. Using empirical pseudopotential calculations of the electronic structure of PbSe NCs, the authors showed that the existence of several valence-band maxima in an energy window of ~ 0.5 eV below the top of the valence band of bulk PbSe results in a denser valence-band manifold compared to the conduction-band manifold.³⁰ On the other hand, recent first-principles calculations for small Pb₁₆Se₁₆ clusters³⁶ found little asymmetry between the densities of states of the valence and conduction bands.

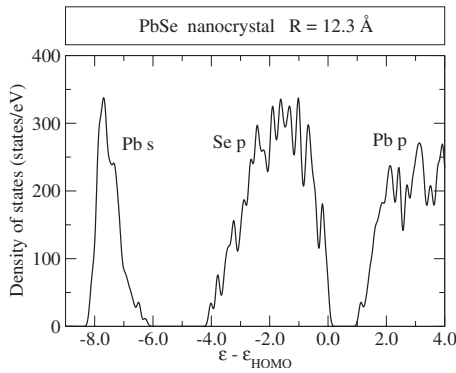


FIG. 4. Density of states of a PbSe NC of radius $R=12.3$ Å. The zero of the energy scale corresponds to the HOMO energy. The energy levels were broadened using a 100-meV-wide Gaussian convolution function.

Figure 4 shows the calculated density of states (DOS) of a $R=12.3$ Å PbSe NC (representative of the other NCs considered here). The narrow band between 6 and 8 eV below the HOMO is due to the Pb 6s levels, which are pulled down into the valence band by relativistic effects.^{41,46} The valence band extends to about 4 eV below the HOMO and is comprised primarily of Se *p* states. The conduction band consists mainly of Pb *p* states. The DOS of PbSe NCs is qualitatively similar to the DOS of bulk PbSe,⁴⁵ although the valence band is narrower (~ 4 eV versus ~ 5 eV in bulk⁴⁵).

To investigate the existence of mirror symmetry between the valence-band and conduction-band manifolds, we show in Fig. 5 the integrated valence-band (VB) and conduction-band (CB) densities of states of the PbSe NCs considered here, plotted as a function of the energy separation from the HOMO and the LUMO energies. The integrated VB DOS $N_V(\epsilon)$ and CB DOS $N_C(\epsilon)$ give the number of single-particle energy levels in the energy intervals $\epsilon_{\text{HOMO}} - \epsilon$ and $\epsilon - \epsilon_{\text{LUMO}}$, respectively. We see from Fig. 5 that $N_V(\epsilon)$ increases at a much faster rate than $N_C(\epsilon)$, meaning that the VB DOS is larger than the CB DOS. For example, for $\epsilon = 0.5$ eV, we find that the ratio N_V/N_C is 1.7 for a $R = 8.4$ Å NC, 2.2 for $R = 12.3$ Å, and 2.5 for $R = 14.8$ Å, whereas the existence of mirror symmetry would imply $N_V/N_C = 1$.

The present results are consistent with the empirical pseudopotential calculations of An *et al.*,³⁰ who found a dense valence-band manifold for $R = 30.6$ Å PbSe NCs. Interestingly, we find that the ratio N_V/N_C at $\epsilon = 0.5$ eV decreases as the NC size decreases, which may explain why Kilina *et al.*³⁶ found little valence-conduction asymmetry in small $\text{Pb}_{16}\text{Se}_{16}$ clusters. Our first-principles calculations suggest that for PbSe NCs of realistic size, there is no mirror

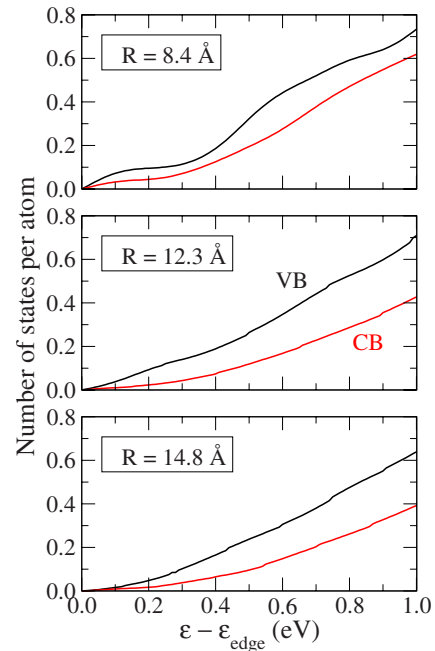


FIG. 5. (Color online) Integrated VB and CB DOS of PbSe NCs, normalized to the number of atoms in the NC. The VB and CB energies are measured from the HOMO and the LUMO, respectively.

symmetry between valence-band and conduction-band levels.

V. CONCLUSIONS

Using first-principles, density-functional-theory calculations, we have investigated the structural and electronic properties of nearly spherical PbSe NCs ranging in radius from 8.4 to 14.8 Å. We found that: (i) The Pb-Se bond lengths and bond angles are significantly distorted compared to those in bulk PbSe, in an ~ 8 -Å-thick shell near the surface of the NC. (ii) Even in the absence of passivants, there are no surface states in the band gap of the NCs. (iii) The band gap undergoes a significant redshift (Franck-Condon shift) upon optical excitation. For NCs of radius $R = 8.4$ Å, the calculated Franck-Condon shift is 0.18 eV. (iv) The calculated electronic density of states shows a significant asymmetry between valence and conduction bands, suggesting that the postulated mirror symmetry between valence and conduction states does not exist.

ACKNOWLEDGMENTS

This work was funded by the U.S. Department of Energy, Office of Science, Basic Energy Sciences, under Contract No. DE-AC36-99GO10337 to NREL.

- ¹R. D. Schaller and V. I. Klimov, *Phys. Rev. Lett.* **92**, 186601 (2004).
- ²R. J. Ellingson, M. C. Beard, J. C. Johnson, P. Yu, O. I. Micic, A. J. Nozik, A. Shabaev, and Al. L. Efros, *Nano Lett.* **5**, 865 (2005).
- ³R. D. Schaller, V. M. Agranovich, and V. I. Klimov, *Nature (London)* **1**, 189 (2005).
- ⁴J. E. Murphy, M. C. Beard, A. G. Norman, S. P. Ahrenkiel, J. C. Johnson, P. Yu, O. I. Mičić, R. J. Ellingson, and A. J. Nozik, *J. Am. Chem. Soc.* **128**, 3241 (2006).
- ⁵J. J. H. Pijpers, E. Hendry, M. T. W. Milder, R. Fanciulli, J. Savolainen, J. L. Herek, D. Vanmaekelbergh, S. Ruhman, D. Mocatta, D. Oron, A. Aharoni, U. Banin, and M. Bonn, *J. Phys. Chem. C* **111**, 4146 (2007).
- ⁶R. D. Schaller, J. M. Pietryga, and V. I. Klimov, *Nano Lett.* **7**, 3469 (2007).
- ⁷M. C. Beard, K. P. Knutsen, P. Yu, J. M. Luther, Q. Song, W. K. Metzger, R. J. Ellingson, and A. J. Nozik, *Nano Lett.* **7**, 2506 (2007).
- ⁸A. Lipovskii, E. Kolobkova, V. Petrikov, I. Kang, A. Olkhovets, T. Krauss, M. Thomas, J. Silcox, F. Wise, Q. Shen, and S. Kucia, *Appl. Phys. Lett.* **71**, 3406 (1997).
- ⁹A. Olkhovets, R. C. Hsu, A. Lipovskii, and F. W. Wise, *Phys. Rev. Lett.* **81**, 3539 (1998).
- ¹⁰B. L. Wehrenberg, C. Wang, and P. Guyot-Sionnest, *J. Phys. Chem. B* **106**, 10634 (2002).
- ¹¹H. Du, C. Chen, R. Krishnan, T. D. Krauss, J. M. Harbold, F. W. Wise, M. G. Thomas, and J. Silcox, *Nano Lett.* **2**, 1321 (2002).
- ¹²B. L. Wehrenberg and P. Guyot-Sionnest, *J. Am. Chem. Soc.* **125**, 7806 (2003).
- ¹³J. M. Pietryga, R. D. Schaller, D. Werder, M. H. Stewart, V. I. Klimov, and J. A. Hollingsworth, *J. Am. Chem. Soc.* **126**, 11752 (2004).
- ¹⁴P. Liljeroth, P. A. Zeijlmans van Emmichoven, S. G. Hickey, H. Weller, B. Grandidier, G. Allan, and D. Vanmaekelbergh, *Phys. Rev. Lett.* **95**, 086801 (2005).
- ¹⁵J. M. Harbold, H. Du, T. D. Krauss, K. S. Cho, C. B. Murray, and F. W. Wise, *Phys. Rev. B* **72**, 195312 (2005).
- ¹⁶E. Lifshitz, M. Brumer, A. Kigel, A. Sashchiuk, M. Bashouti, M. Sirota, E. Galun, Z. Burshtein, A. LeQuang, I. Ledoux-Rak, and J. Zyss, *J. Phys. Chem. B* **110**, 25356 (2006).
- ¹⁷R. D. Schaller, J. M. Pietryga, S. V. Goupalov, M. A. Petruska, S. A. Ivanov, and V. I. Klimov, *Phys. Rev. Lett.* **95**, 196401 (2005).
- ¹⁸K. K. Zhuravlev, J. M. Pietryga, R. K. Sander, and V. I. Klimov, *Appl. Phys. Lett.* **90**, 043110 (2007).
- ¹⁹C. Bonati, A. Cannizzo, D. Tonti, A. Tortschanoff, F. van Mourik, and M. Chergui, *Phys. Rev. B* **76**, 033304 (2007).
- ²⁰J. M. Harbold and F. W. Wise, *Phys. Rev. B* **76**, 125304 (2007).
- ²¹I. Moreels, K. Lambert, D. De Muynck, F. Vanhaecke, D. Poelman, J. C. Martins, G. Allan, and Z. Hens, *Chem. Mater.* **19**, 6101 (2007).
- ²²J. M. Luther, M. Law, Q. Song, C. L. Perkins, M. C. Beard, and A. J. Nozik, *ACS Nano* **2**, 271 (2008).
- ²³R. Koole, G. Allan, C. Delerue, A. Meijerink, D. Vanmaekelbergh, and A. J. Houtepen, *Small* **4**, 127 (2008).
- ²⁴I. Kang and F. W. Wise, *J. Opt. Soc. Am. B* **14**, 1632 (1997).
- ²⁵A. D. Andreev and A. A. Lipovskii, *Phys. Rev. B* **59**, 15402 (1999).
- ²⁶G. E. Tudury, M. V. Marquezini, L. G. Ferreira, L. C. Barbosa, and C. L. Cesar, *Phys. Rev. B* **62**, 7357 (2000).
- ²⁷A. C. Bartnik, F. W. Wise, A. Kigel, and E. Lifshitz, *Phys. Rev. B* **75**, 245424 (2007).
- ²⁸G. Allan and C. Delerue, *Phys. Rev. B* **70**, 245321 (2004).
- ²⁹G. Allan and C. Delerue, *Phys. Rev. B* **73**, 205423 (2006).
- ³⁰J. M. An, S. V. Dudiy, A. Franceschetti, and A. Zunger, *Nano Lett.* **6**, 2728 (2006).
- ³¹A. Franceschetti, J. M. An, and A. Zunger, *Nano Lett.* **6**, 2191 (2006).
- ³²A. Shabaev, Al. L. Efros, and A. J. Nozik, *Nano Lett.* **6**, 2856 (2006).
- ³³J. M. An, A. Franceschetti, and A. Zunger, *Phys. Rev. B* **76**, 045401 (2007).
- ³⁴J. M. An, A. Franceschetti, and A. Zunger, *Nano Lett.* **7**, 2129 (2007).
- ³⁵H. Kamisaka, S. V. Kilina, K. Yamashita, and O. V. Prezhdo, *Nano Lett.* **6**, 2295 (2006).
- ³⁶S. V. Kilina, C. F. Craig, D. Kilin, and O. V. Prezhdo, *J. Phys. Chem. C* **111**, 4871 (2007).
- ³⁷J. M. An, A. Franceschetti, and A. Zunger, *Phys. Rev. B* **76**, 161310(R) (2007).
- ³⁸J. M. An, M. Califano, A. Franceschetti, and A. Zunger, *J. Chem. Phys.* **128**, 164720 (2008).
- ³⁹*Semiconductors. II-VI and I-VII Compounds; Semimagnetic Compounds*, edited by U. Rossler, Landolt-Börnstein, New Series, Group III, Vol. 41 (Springer-Verlag, Berlin, 2001).
- ⁴⁰Al. L. Efros, V. A. Karchenko, and M. Rosen, *Solid State Commun.* **93**, 281 (1995).
- ⁴¹S. H. Wei and A. Zunger, *Phys. Rev. B* **55**, 13605 (1997).
- ⁴²G. Kresse and J. Fürthmüller, *Comput. Mater. Sci.* **6**, 15 (1996).
- ⁴³J. P. Perdew, K. Burke, and M. Ernzerhof, *Phys. Rev. Lett.* **77**, 3865 (1996).
- ⁴⁴P. E. Blöchl, *Phys. Rev. B* **50**, 17953 (1994).
- ⁴⁵E. A. Albanesi, C. M. I. Okoye, C. O. Rodriguez, E. L. Peltzer y Blanca, and A. G. Petukhov, *Phys. Rev. B* **61**, 16589 (2000).
- ⁴⁶A. Franceschetti and S. T. Pantelides, *Phys. Rev. B* **68**, 033313 (2003).
- ⁴⁷K. Hummer, A. Grüneis, and G. Kresse, *Phys. Rev. B* **75**, 195211 (2007).
- ⁴⁸G. Allan, *Phys. Rev. B* **43**, 9594 (1991).
- ⁴⁹A. Franceschetti, *Phys. Rev. B* **76**, 161301(R) (2007).
- ⁵⁰A. A. Lazarides, C. B. Duke, A. Paton, and A. Kahn, *Phys. Rev. B* **52**, 14895 (1995).
- ⁵¹A. Satta and S. de Gironcoli, *Phys. Rev. B* **63**, 033302 (2000).
- ⁵²J. Ma, Y. Jia, Y. Song, E. Liang, L. Wu, F. Wang, X. Wang, and X. Hu, *Surf. Sci.* **551**, 91 (2004).
- ⁵³V. Perebeinos, S. W. Chan, and F. Zhang, *Solid State Commun.* **123**, 295 (2002).
- ⁵⁴A. Puzder, A. J. Williamson, F. Gygi, and G. Galli, *Phys. Rev. Lett.* **92**, 217401 (2004).
- ⁵⁵A. Puzder, A. J. Williamson, J. C. Grossman, and G. Galli, *J. Am. Chem. Soc.* **125**, 2786 (2003).
- ⁵⁶E. Degoli, G. Cantele, E. Luppi, R. Magri, D. Ninno, O. Bisi, and S. Ossicini, *Phys. Rev. B* **69**, 155411 (2004).
- ⁵⁷F. Iori, E. Degoli, R. Magri, I. Marri, G. Cantele, D. Ninno, F. Trani, O. Pulci, and S. Ossicini, *Phys. Rev. B* **76**, 085302 (2007).